Supplementary Materials

This document provides supplementary information for the manuscript "The Ortholog Conjecture Revisited: the Value of Orthologs and Paralogs in Function Prediction" by Moses Stamboulian, Rafael F. Guerrero, Matthew W. Hahn, and Predrag Radivojac. The manuscript appears in *Bioinformatics*, 2020.

Maryland bridge similarity. Let A and B be two sets of GO terms denoting the propagated functional annotations for the proteins a and b, respectively. The Maryland bridge similarity [1] is defined as

$$s_{\mathrm{M}}(A, B) = \frac{1}{2} \cdot \left(\frac{|A \cap B|}{|A|} + \frac{|A \cap B|}{|B|} \right), \tag{1}$$

and can be interpreted as an average of precision and recall when the terms associated with protein a are used as a prediction of the terms associated with protein b, and *vice versa*. The root term was excluded from these calculations, in order to exploit the full $[0, 1]$ range for functional similarity.

Schlicker semantic similarity. The Schlicker similarity used here is a slight modification of the original similarity measure [2], as proposed in [3]. To calculate the similarity between two leaf GO terms, t_i and t_j, this measure uses Lin's similarity measure defined as

$$s_{\mathrm{L}}(t_i, t_j) = \frac{2 \cdot s_{\mathrm{R}}(t_i, t_j)}{\log {}^{1}\!/_{P(t_i)} + \log {}^{1}\!/_{P(t_j)}}, \tag{2}$$

where $P(t)$ is the probability of observing a term t in a randomly selected protein, and $s_{\mathrm{R}}(t_i, t_j)$ is Resnik's similarity [4] between the terms, calculated as

$$s_{\mathrm{R}}(t_i, t_j) = \max_{t \in \mathcal{A}(t_i, t_j)} \frac{1}{\log P(t)}. \tag{3}$$

In Eq. (3), $\mathcal{A}(t_i, t_j)$ indicates the set of common ancestor terms between terms t_i and t_j in the ontology. Term probabilities were estimated using their relative frequencies in the annotations of all species in the UniProt-GOA database.

As gene products are often annotated with more than one leaf term, functional similarity for a protein pair was calculated using the best match average method, proposed originally in Schlicker et al. [2], giving the following Schlicker similarity

$$s_{\mathrm{S}} = \frac{1}{|p_1| + |p_2|} \cdot \left(\sum_{i \in p_1} \max_{j \in p_2} (s_{\mathrm{L}}(i, j)) + \sum_{j \in p_2} \max_{i \in p_1} (s_{\mathrm{L}}(i, j)) \right) \tag{4}$$

Combining the terms in Eq. (4) differs from the original formula suggested in [2] in the way that the two maximum terms are averaged. This particular implementation was chosen to closely match the semantic similarity from [3].

Topological metrics. The performance of protein function prediction was evaluated using a leave-one-out strategy based on one topological and one information-theoretic accuracy measure. We used the $F_{\max}$ topological metric, a criterion regularly seen in CAFA [5, 6, 7]. To summarize this performance evaluation process, we consider a prediction algorithm on a set of n proteins, where each protein i is assigned a score (say, between 0 and 1) for each functional term v in the ontology. We now define an average precision (pr) and recall (rc) at some score threshold τ as

$$pr(\tau) = \frac{1}{m(\tau)} \sum_{i=1}^{m(\tau)} \frac{\sum_v \mathbb{1}(v \in P_i(\tau) \wedge v \in T_i)}{\sum_v \mathbb{1}(v \in P_i(\tau))} \tag{5}$$

$$rc(\tau) = \frac{1}{n} \sum_{i=1}^{n} \frac{\sum_v \mathbb{1}(v \in P_i(\tau) \wedge v \in T_i)}{\sum_v \mathbb{1}(v \in T_i)}, \tag{6}$$

where $P_i(\tau)$ contains predicted terms with a score greater than or equal to τ for the i-th protein, T_i is the experimental annotation for the i-th protein, $m(\tau)$ is the number of proteins having at least one annotation transferred with a score greater than or equal to τ, and $\mathbb{1}$ is an indicator function. The $F_{\max}$ score is defined as

$$F_{\max} = \max_{\tau} \left\{ \frac{2 \cdot pr(\tau) \cdot rc(\tau)}{pr(\tau) + rc(\tau)} \right\} \tag{7}$$

and represents the maximum harmonic mean between average precision and average recall over all thresholds.

Supplementary Figures

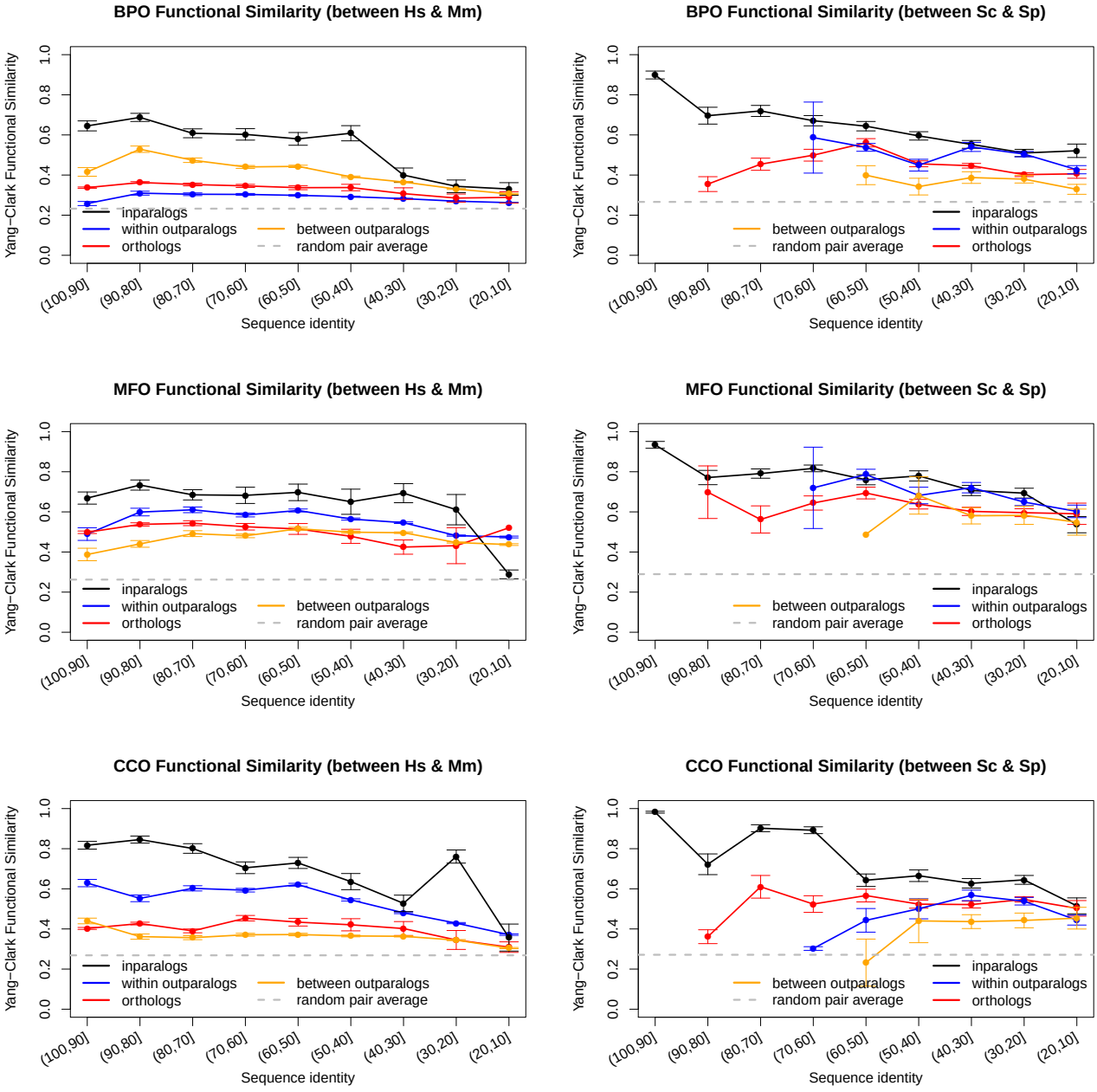

Figure S1: Relationship between functional similarity and sequence identity for human-mouse and cerevisiae-pombe homologs for all three ontologies, using Yang-Clark similarity, with species specific annotations.

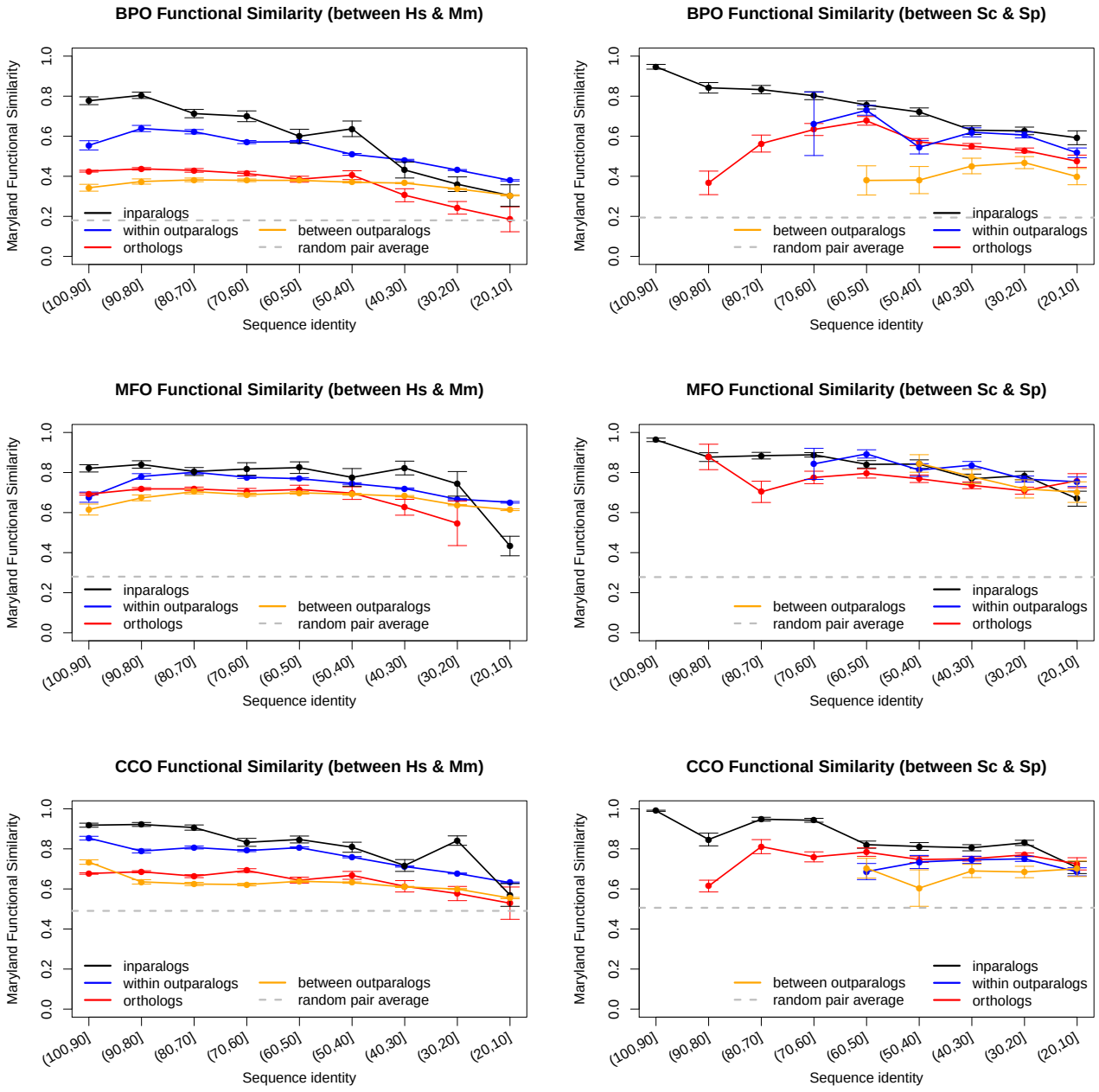

Figure S2: Relationship between functional similarity and sequence identity for human-mouse and cerevisiae-pombe homologs for all three ontologies, using Maryland bridge similarity.

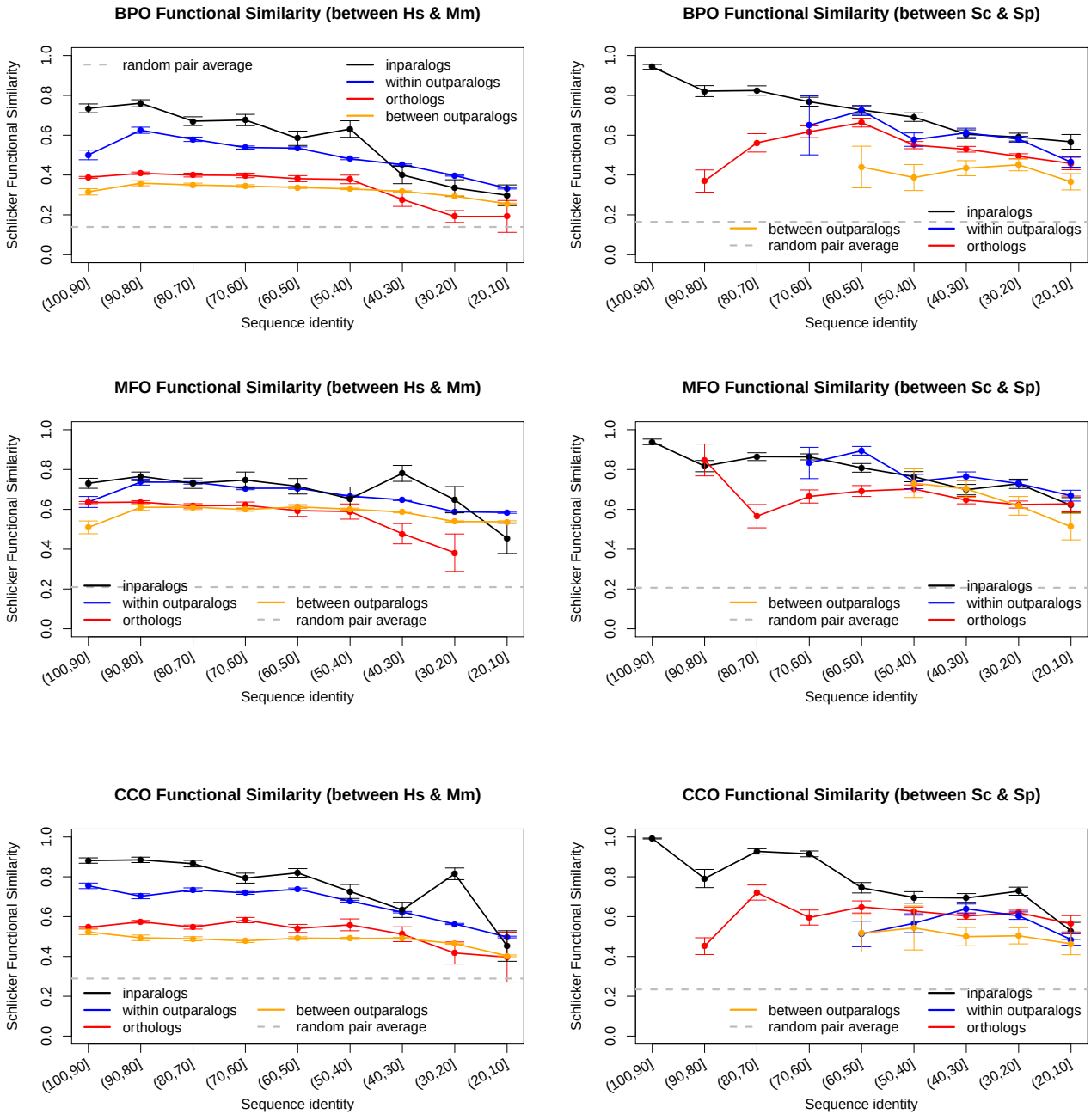

Figure S3: Relationship between functional similarity and sequence identity for human-mouse and cerevisiae-pombe homologs for all three ontologies, using Schlicker's similarity.

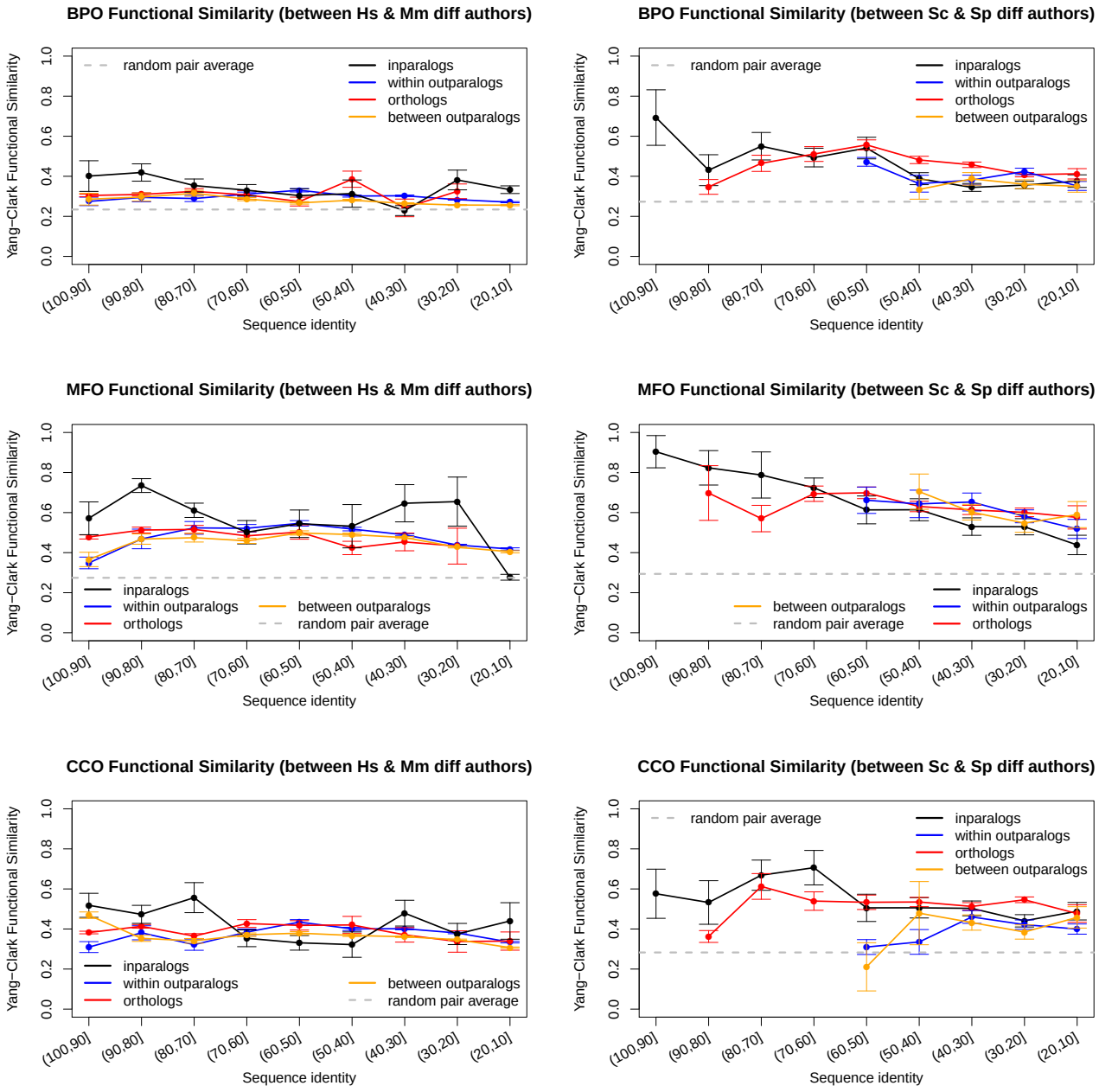

Figure S4: Relationship between functional similarity and sequence identity for human-mouse and cerevisiae-pombe pairs annotated by different authors, for all three ontologies, using Yang-Clark similarity.

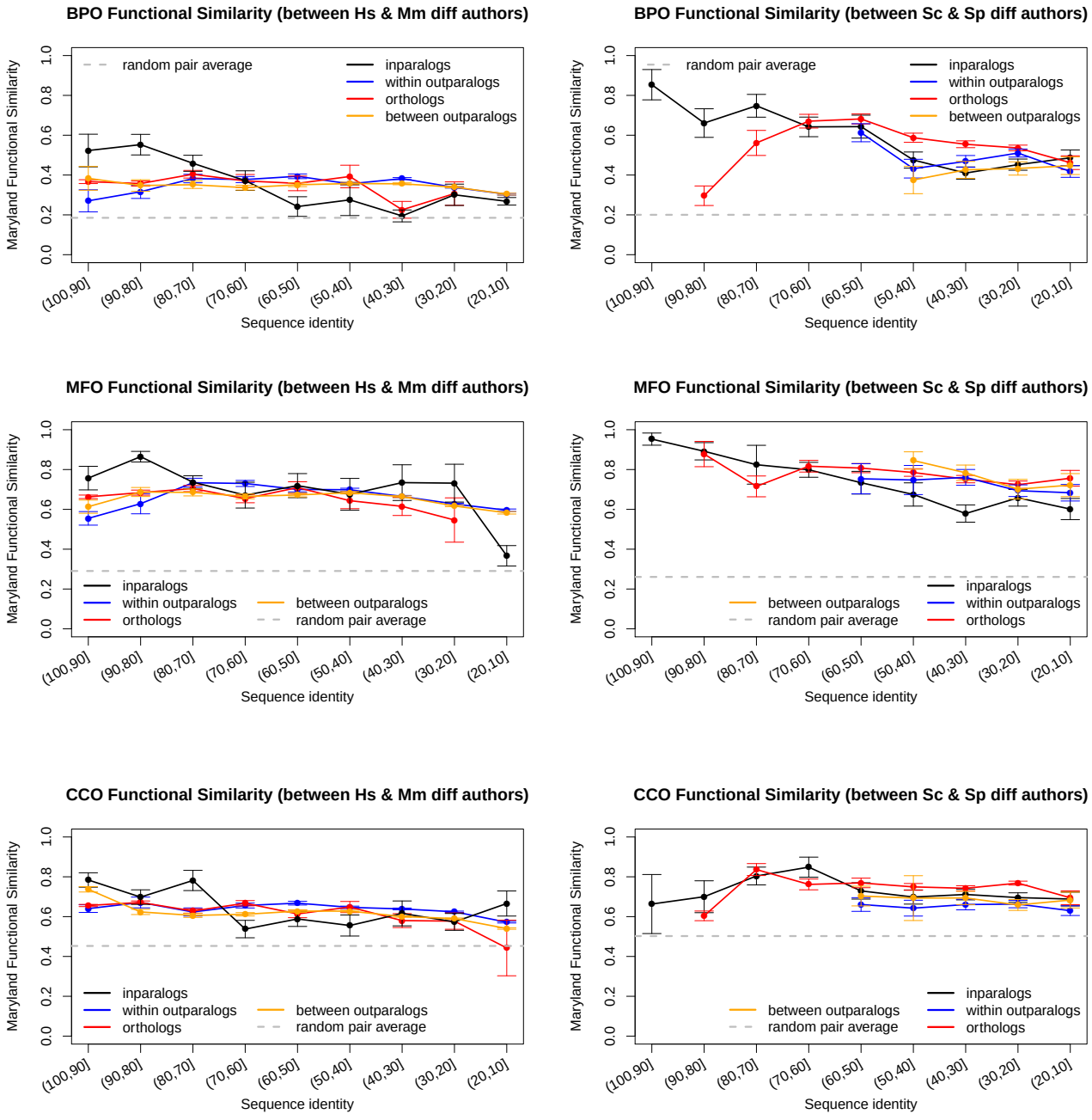

Figure S5: Relationship between functional similarity and sequence identity for human-mouse and cerevisiae-pombe pairs annotated by different authors, for all three ontologies, using Maryland bridge similarity.

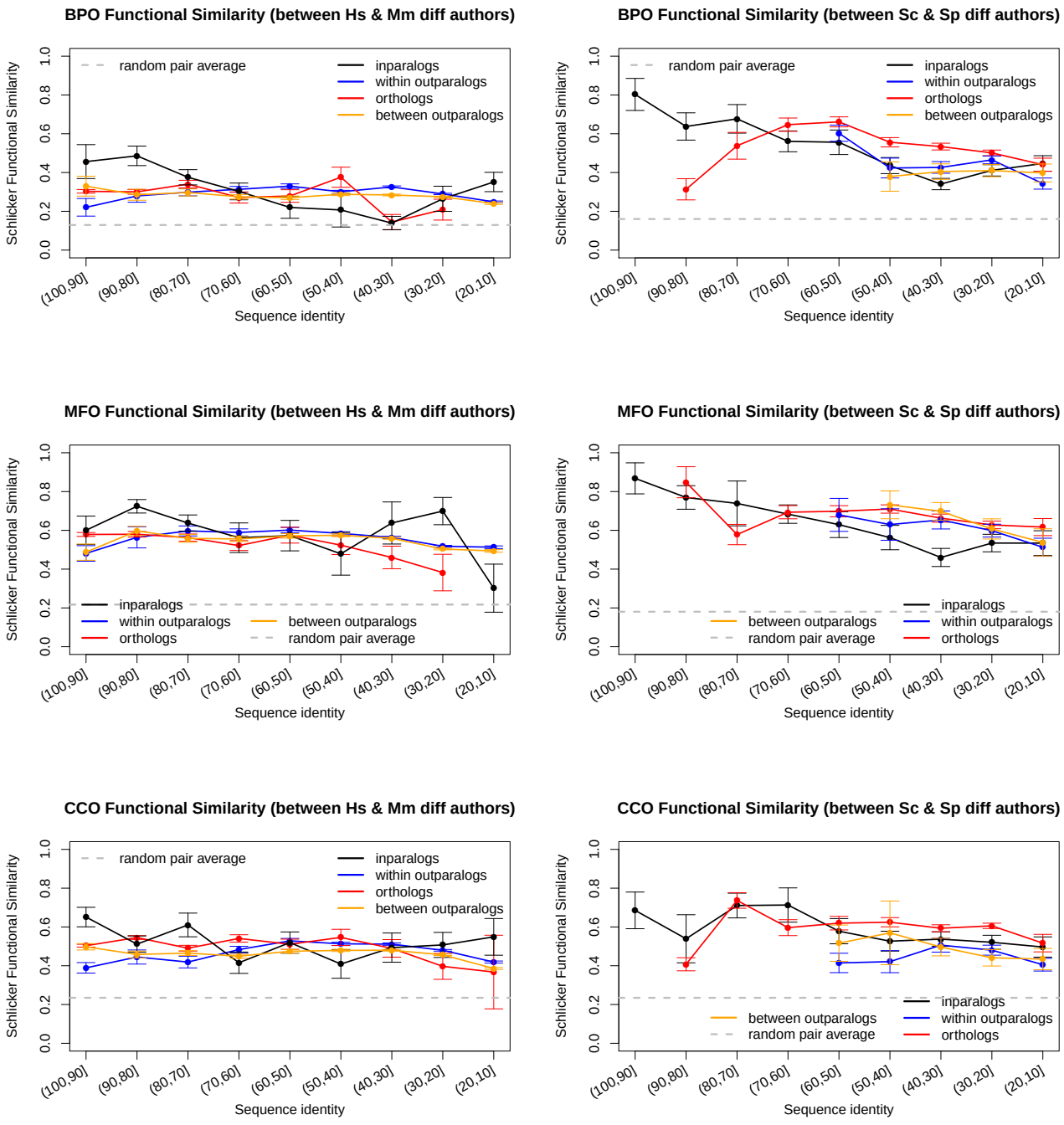

Figure S6: Relationship between functional similarity and sequence identity for human-mouse and cerevisiae-pombe pairs annotated by different authors, for all three ontologies, using Schlicker's similarity.

Figure S7: Background similarity for different types of homology relationships for human-mouse (left panels) and cerevisiae-pombe (right panels), using Yang-Clark similarity.

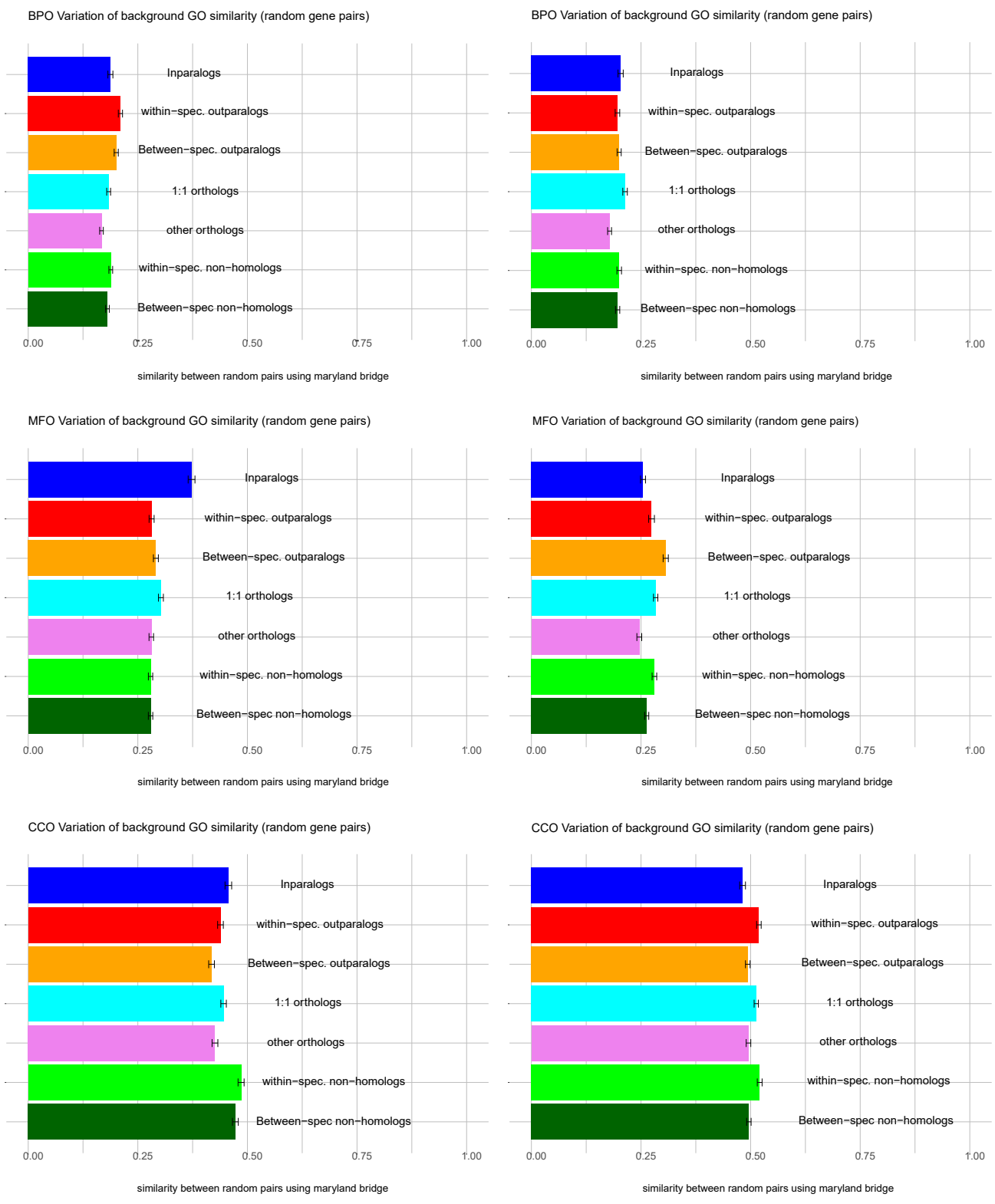

Figure S8: Background similarity for different types of homology relationships for human-mouse (left panels) and cerevisiae-pombe (right panels), using Maryland bridge similarity.

Figure S9: Background similarity for different types of homology relationships for human-mouse (left panels) and cerevisiae-pombe (right panels), using Schlicker's similarity.

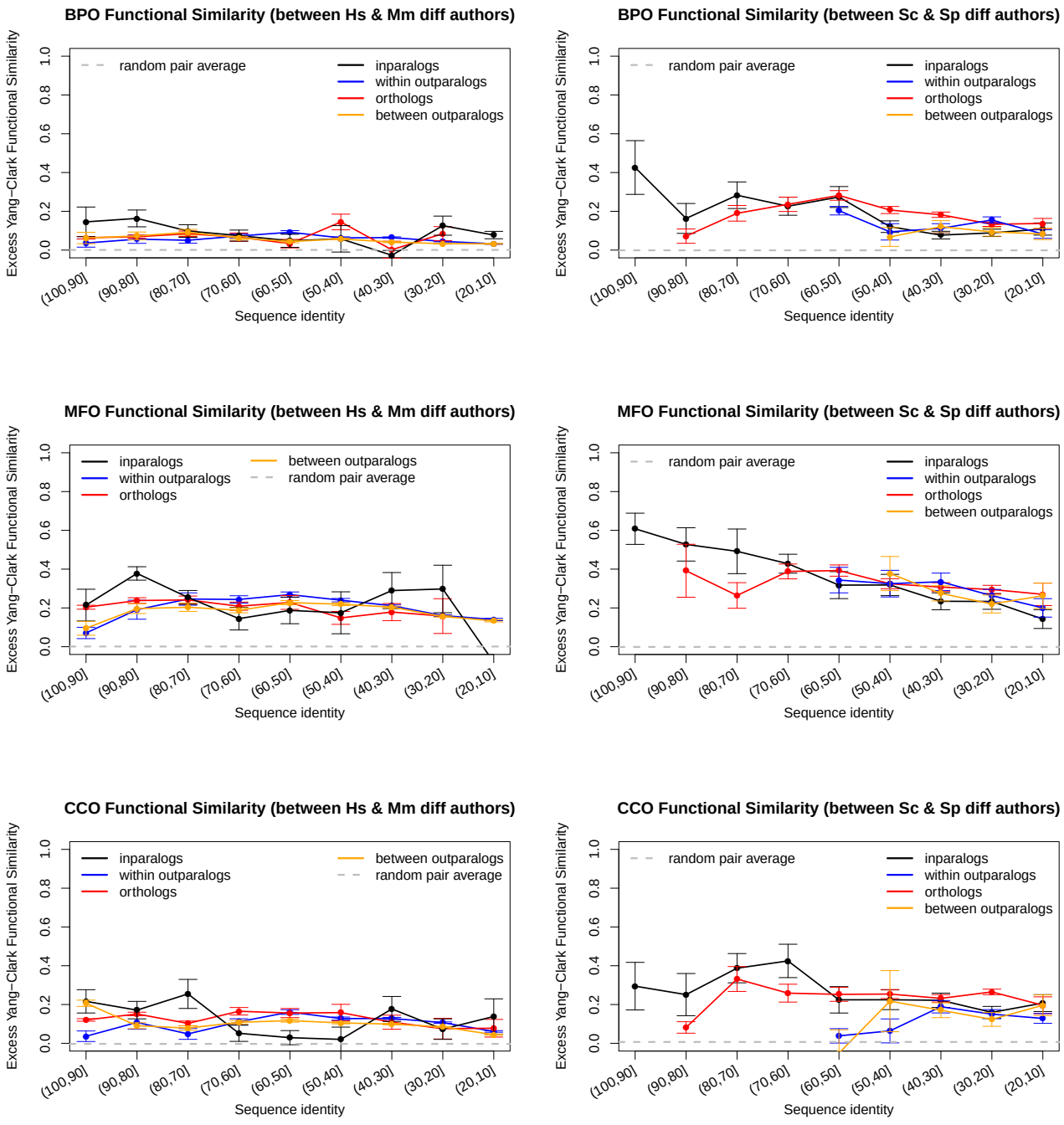

Figure S10: Relationship between functional similarity and sequence identity for human-mouse and cerevisiae-pombe pairs annotated by different authors after removing background similarities, for all three ontologies, using Yang-Clark similarity.

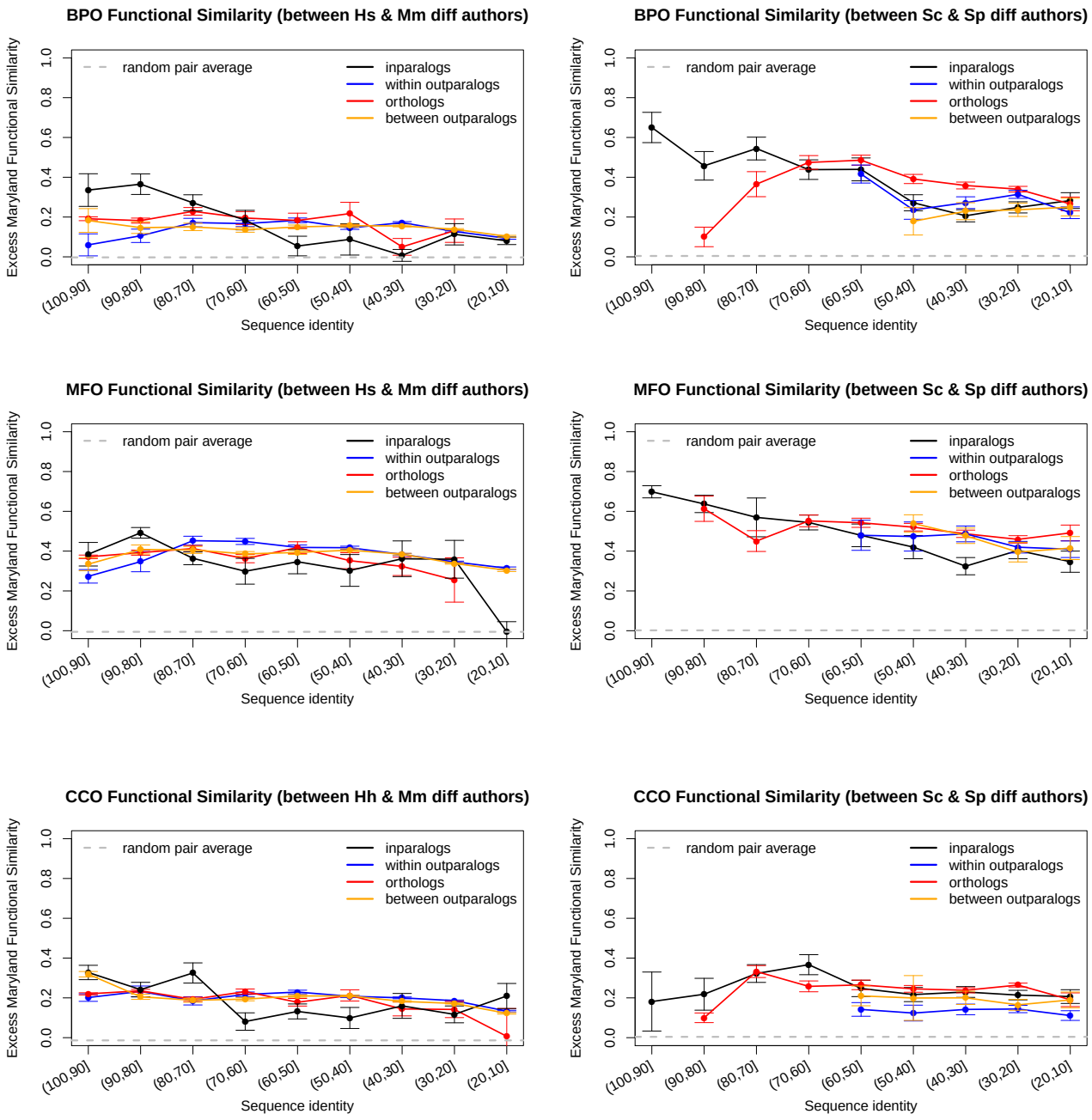

Figure S11: Relationship between functional similarity and sequence identity for human-mouse and cerevisiae-pombe pairs annotated by different authors after removing background similarities, for all three ontologies, using Maryland bridge similarity.

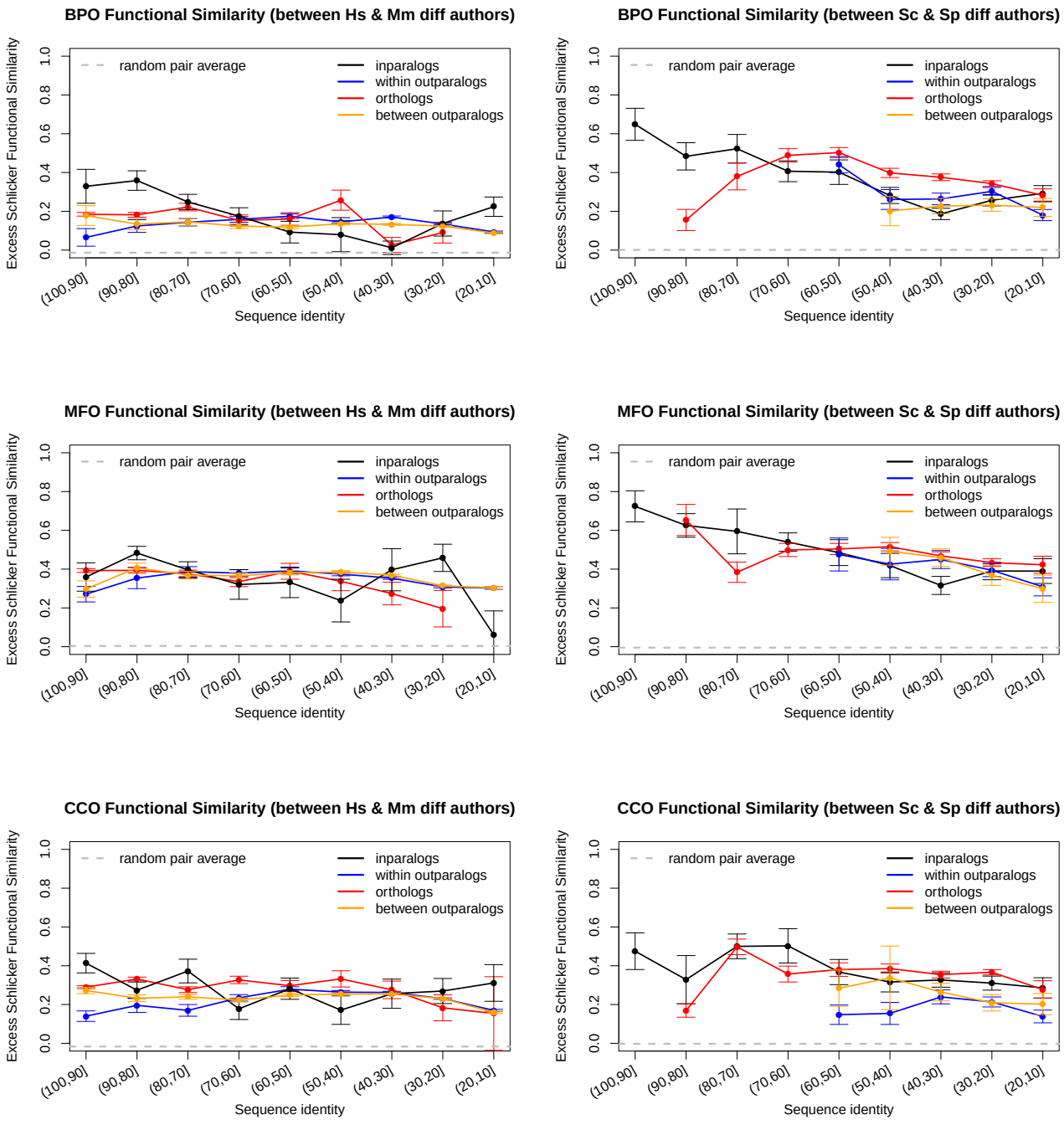

Figure S12: Relationship between functional similarity and sequence identity for human-mouse and cerevisiae-pombe pairs annotated by different authors after removing background similarity, for all three ontologies, using Schlicker's similarity.

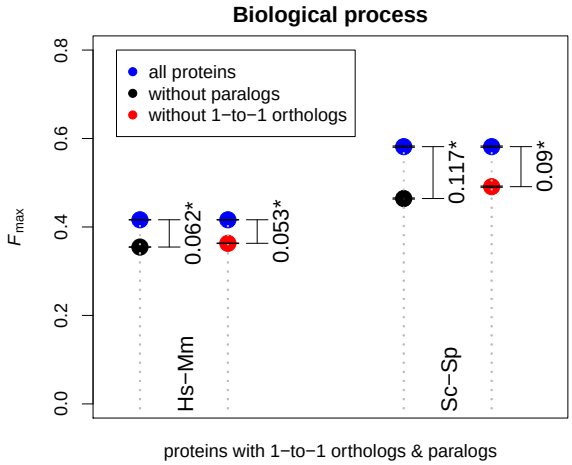

(a)

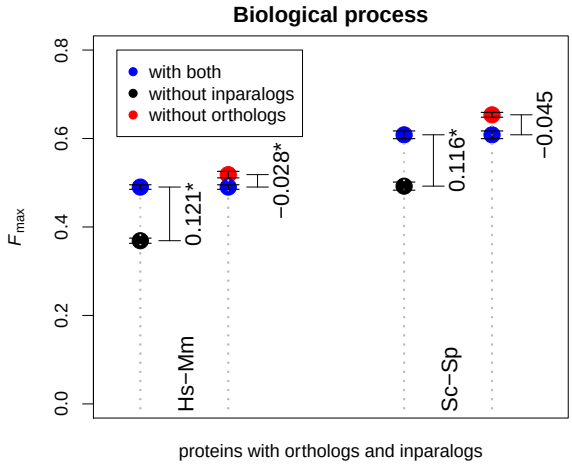

(b)

Figure S13: $F_{\max}$ values for proteins having orthologs, proteins having orthologs and other homologs (a) and proteins having 1-to-1 orthologs and paralogs (b) in human-mouse and cerevisiae-pombe using biological process ontology (* indicates values are statistically significant).

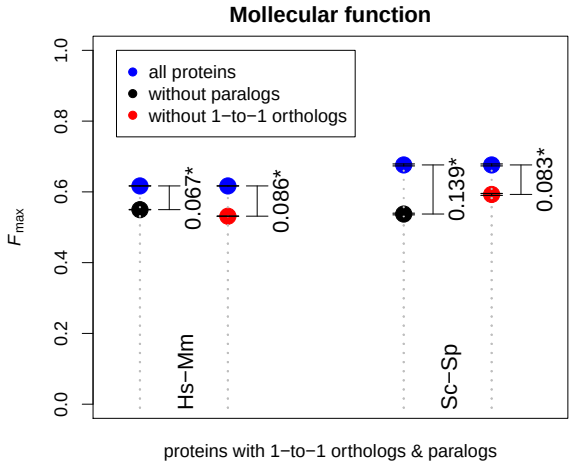

(a)

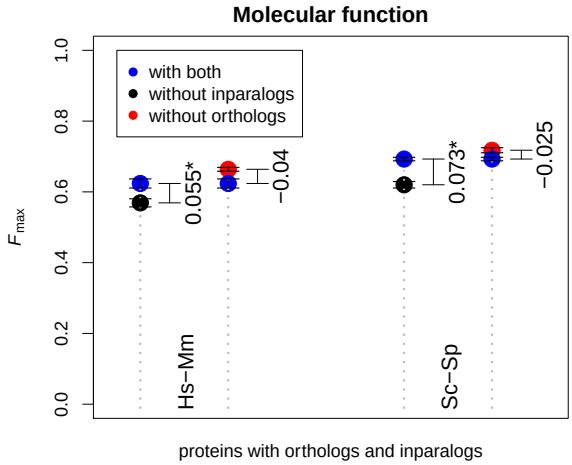

(b)

Figure S14: $F_{\max}$ values for proteins having orthologs, proteins having orthologs and other homologs (a) and proteins having 1-to-1 orthologs and paralogs (b) in human-mouse and cerevisiae-pombe using molecular function ontology (* indicates values are statistically significant).

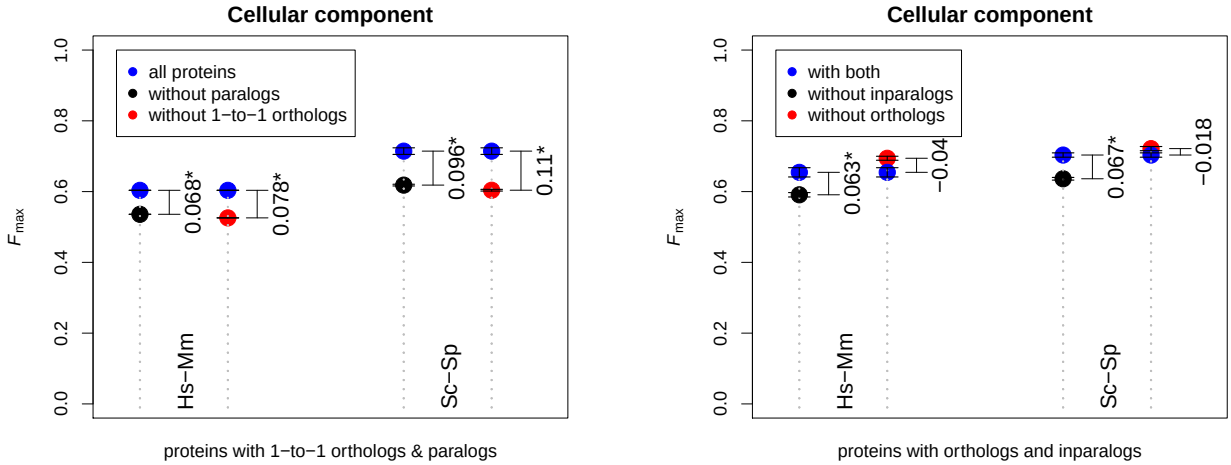

(a) (b)

Figure S15: $F_{\max}$ values for proteins having orthologs, proteins having orthologs and other homologs (a) and proteins having 1-to-1 orthologs and paralogs (b) in human-mouse and cerevisiae-pombe using cellular context ontology (* indicates values are statistically significant).

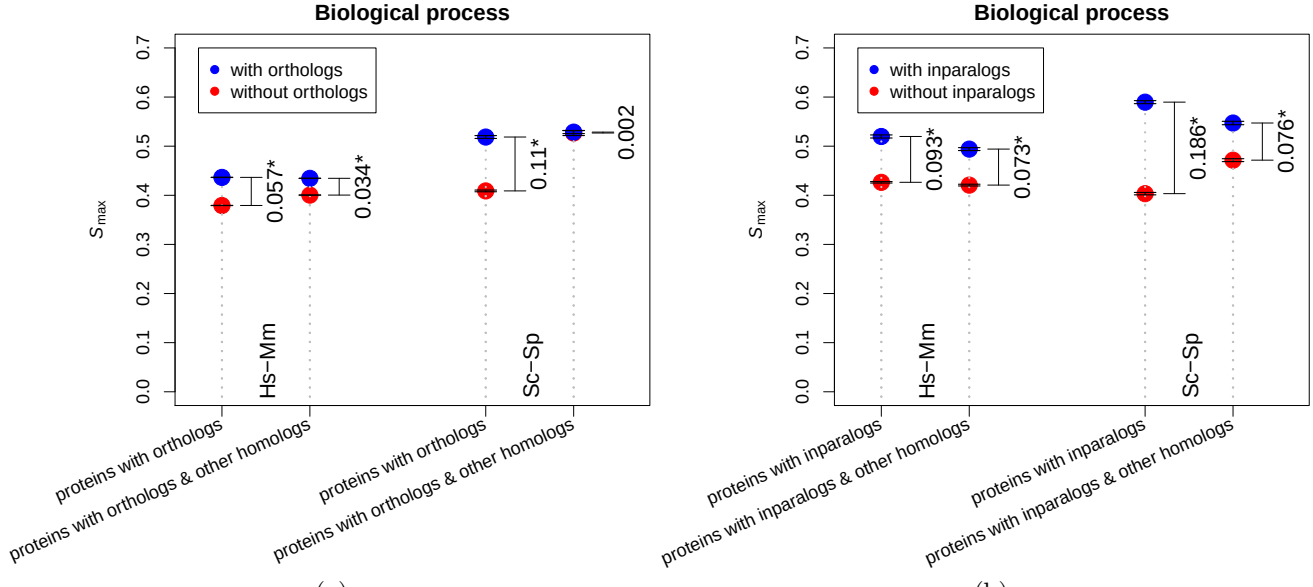

(a) (b)

Figure S16: $S_{\max}$ values for proteins having inparalogs, proteins having inparalogs and other homologs (a), and proteins having both inparalogs and orthologs (b) in human-mouse and cerevisiae-pombe using biological process ontology (* indicates values are statistically significant).

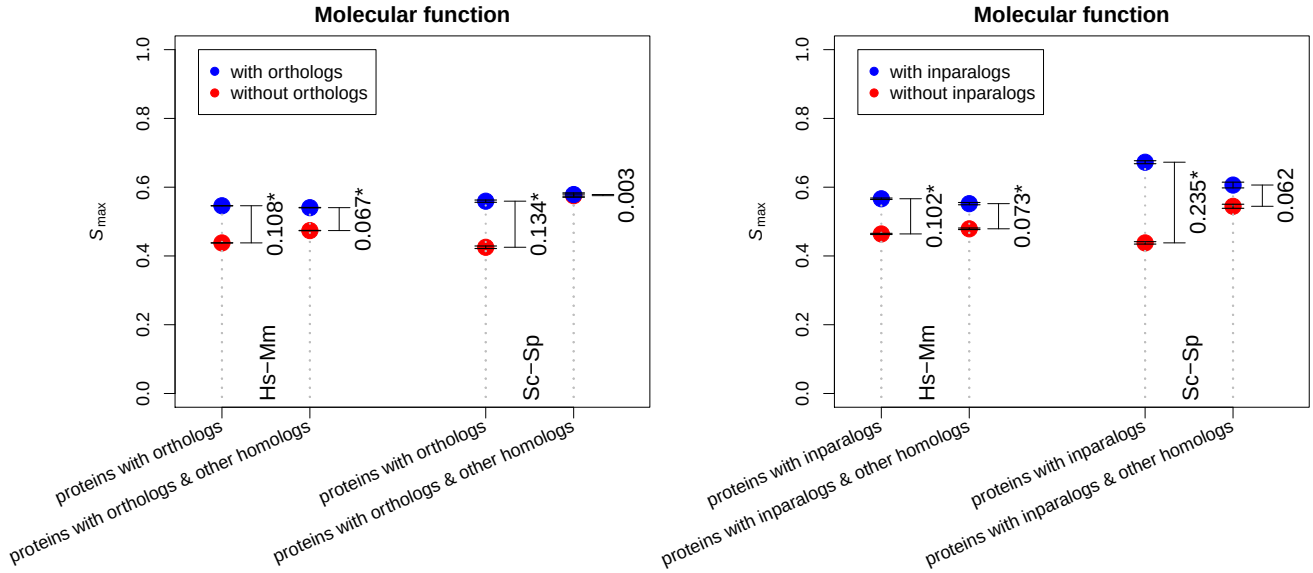

(a) (b)

Figure S17: $S_{\max}$ values for proteins having inparalogs, proteins having inparalogs and other homologs (a), and proteins having both inparalogs and orthologs (b) in human-mouse and cerevisiae-pombe using molecular function ontology (* indicates values are statistically significant).

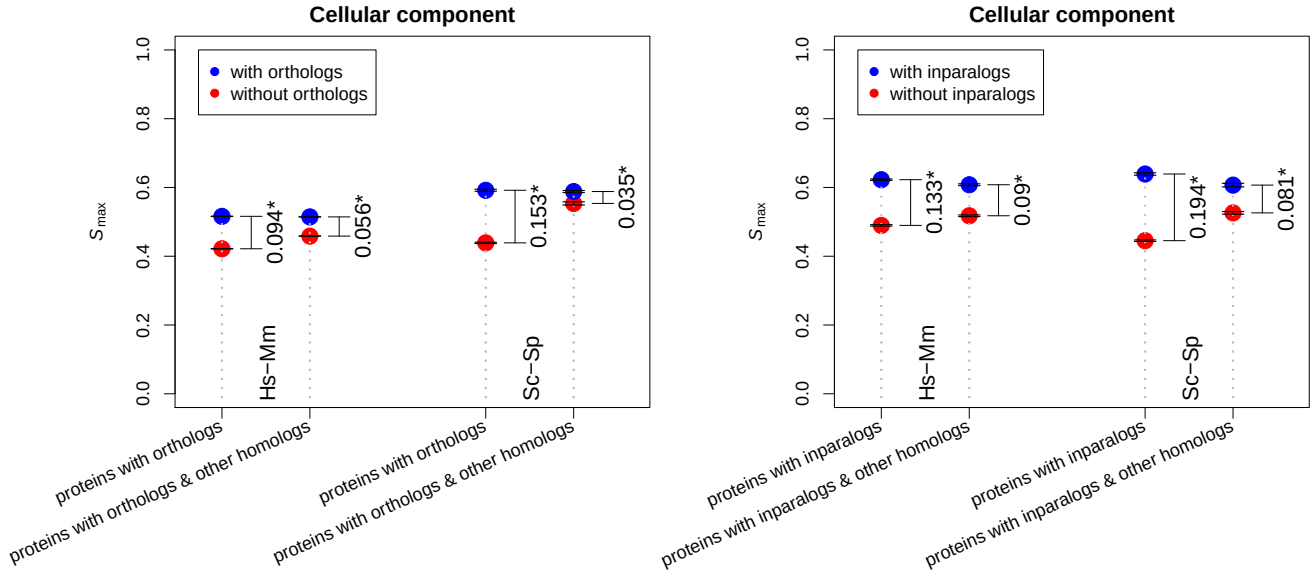

(a) (b)

Figure S18: $S_{\max}$ values for proteins having inparalogs, proteins having inparalogs and other homologs (a), and proteins having both inparalogs and orthologs (b) in human-mouse and cerevisiae-pombe using cellular context ontology (* indicates values are statistically significant).

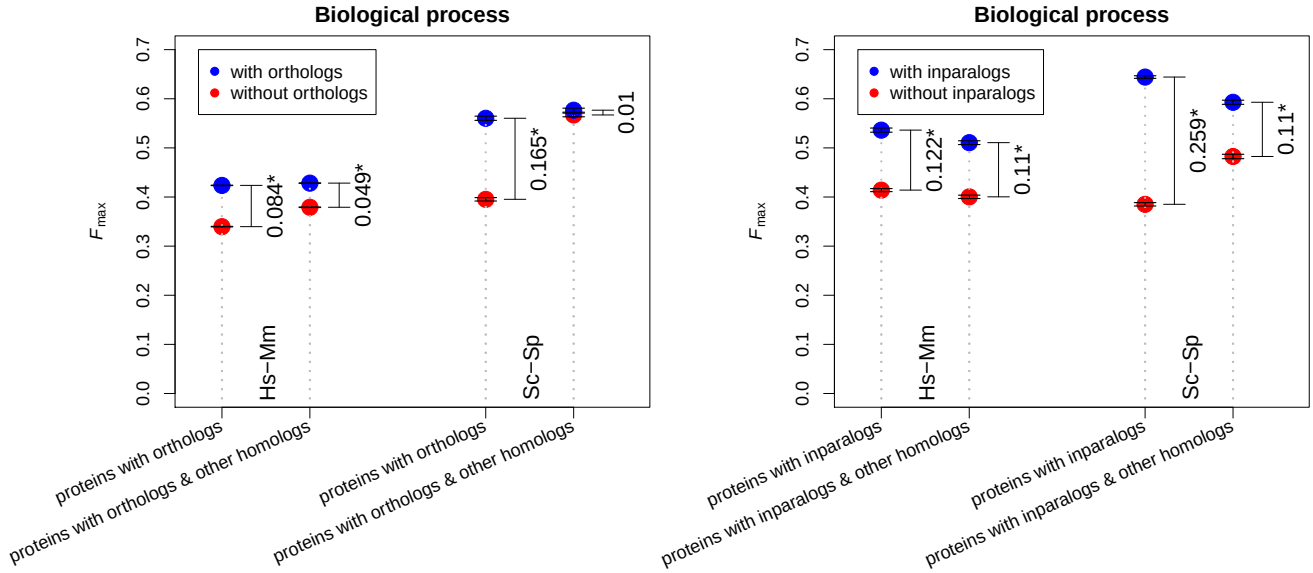

(a) (b)

Figure S19: $F_{\max}$ values for proteins having inparalogs, proteins having inparalogs and other homologs (a), and proteins having both inparalogs and orthologs (b) in human-mouse and cerevisiae-pombe using biological process ontology (* indicates values are statistically significant).

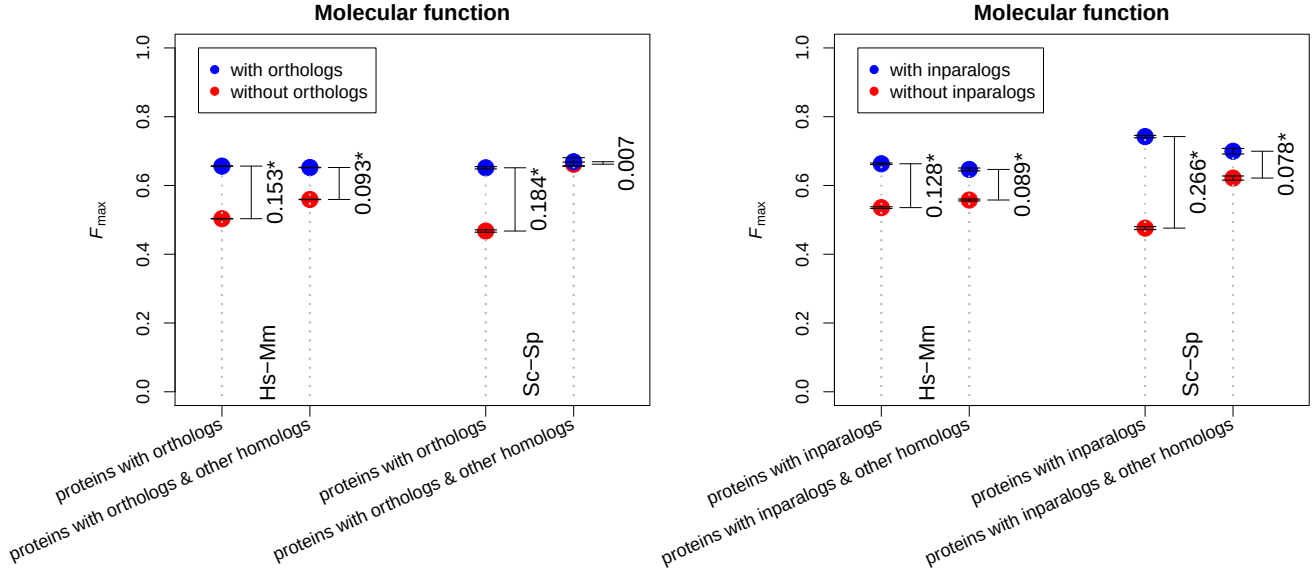

(a) (b)

Figure S20: $F_{\max}$ values for proteins having inparalogs, proteins having inparalogs and other homologs (a), and proteins having both inparalogs and orthologs (b) in human-mouse and cerevisiae-pombe using molecular function ontology (* indicates values are statistically significant).

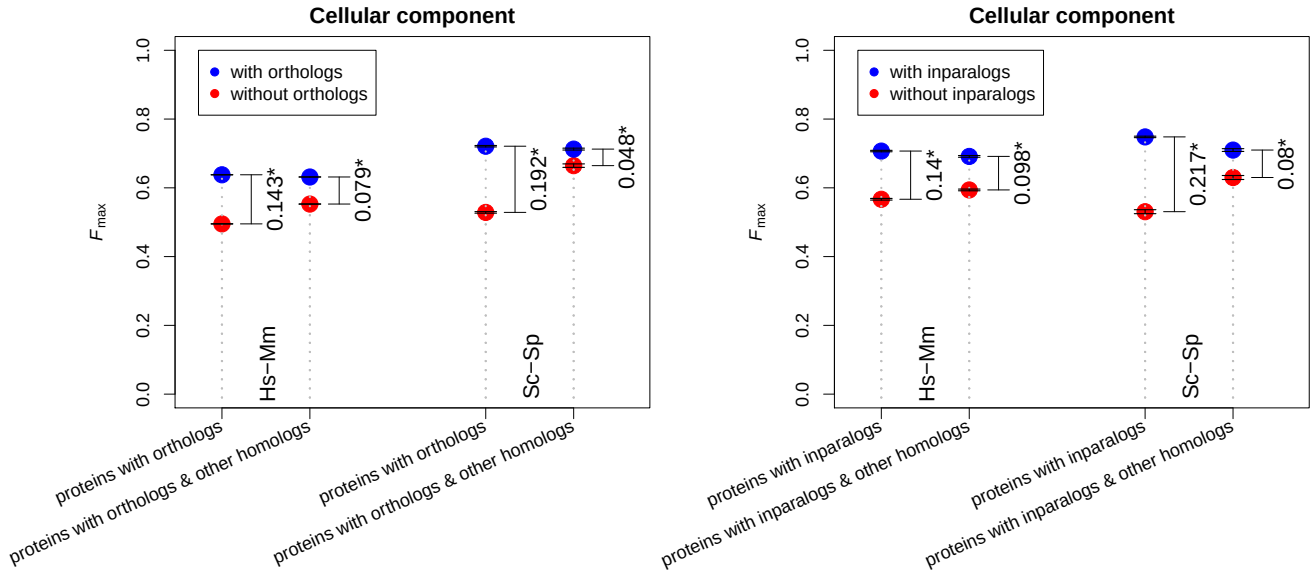

(a) (b)

Figure S21: $F_{\max}$ values for proteins having inparalogs, proteins having inparalogs and other homologs (a), and proteins having both inparalogs and orthologs (b) in human-mouse and cerevisiae-pombe using cellular context ontology (* indicates values are statistically significant).

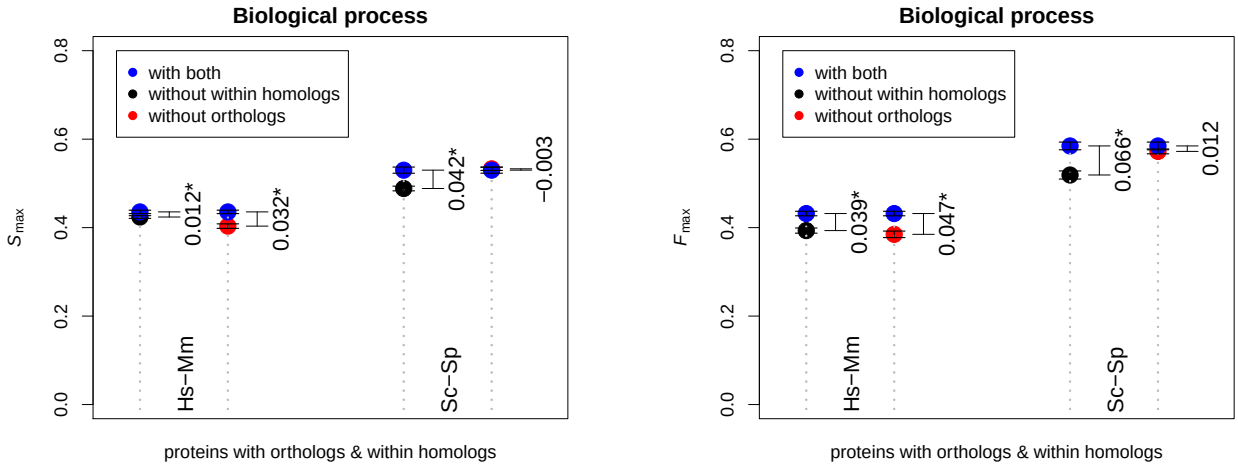

(a) (b)

Figure S22: $S_{\max}$ values for proteins both orthologs and within species homologs (a), Fmax values for proteins having both orthologs and within species homologs in human-mouse and cerevisiae-pombe using biological process ontology (* indicates values are statistically significant).

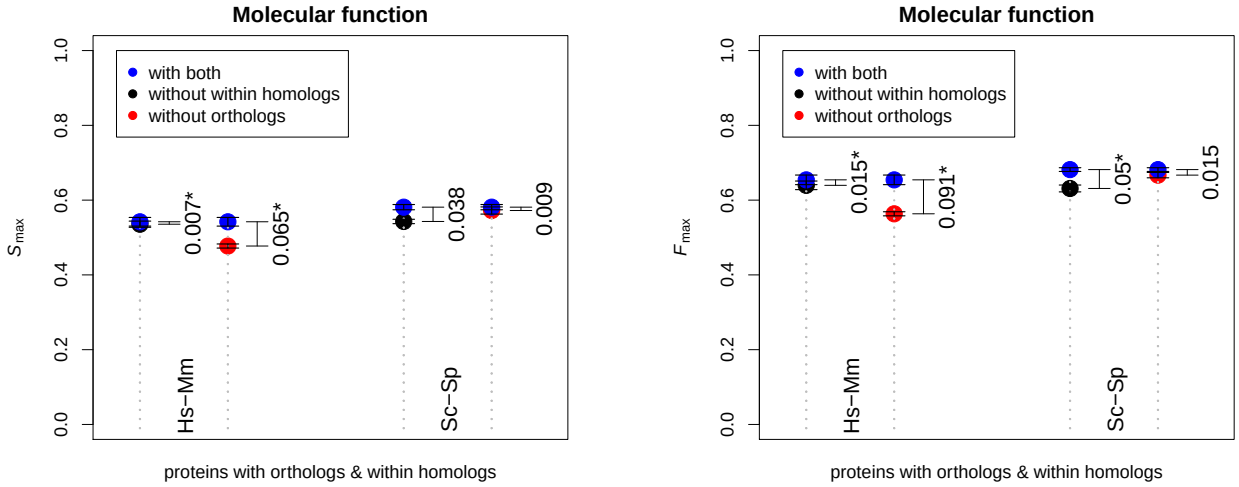

(a) (b)

Figure S23: $S_{\max}$ values for proteins both orthologs and within species homologs (a), Fmax values for proteins having both orthologs and within species homologs in human-mouse and cerevisiae-pombe using molecular function ontology (* indicates values are statistically significant).

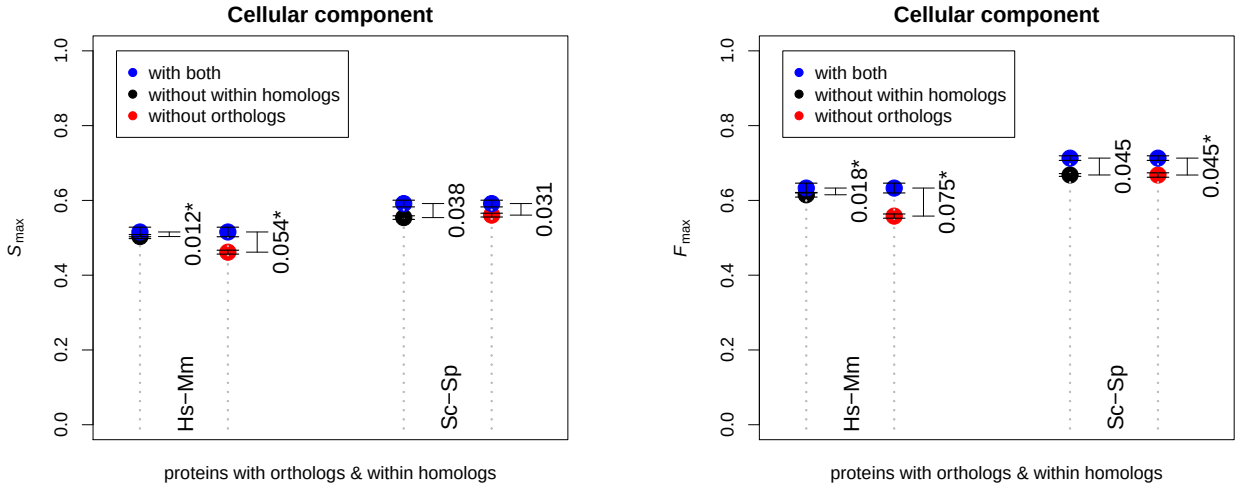

(a) (b)

Figure S24: $S_{\max}$ values for proteins both orthologs and within species homologs (a), Fmax values for proteins having both orthologs and within species homologs in human-mouse and cerevisiae-pombe using cellular context ontology (* indicates values are statistically significant).

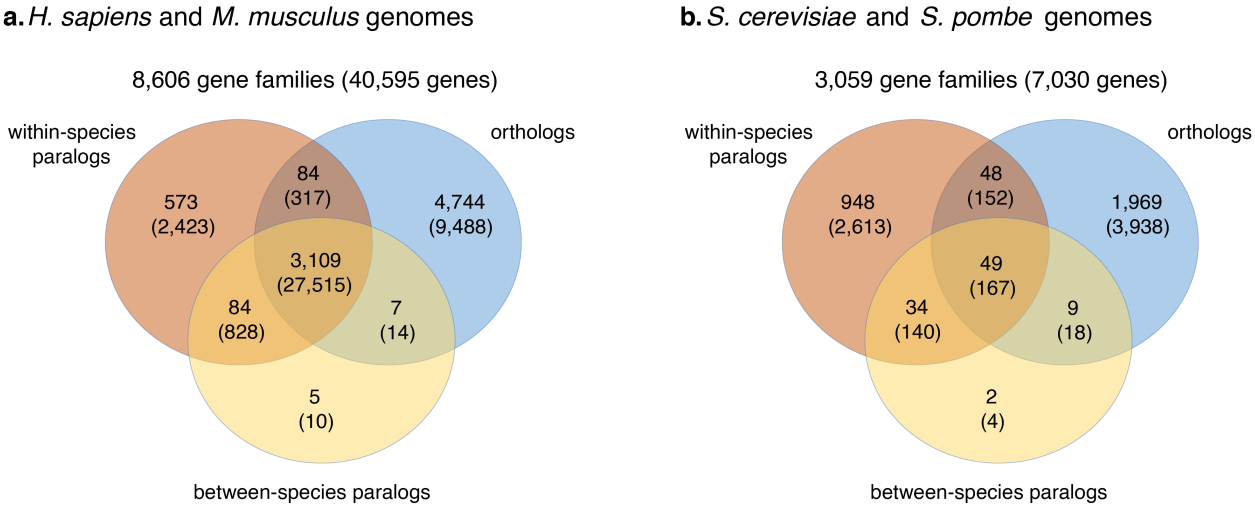

Figure S25: The numbers of gene families with different types of homologous relationships in them, where orthologs represent only one-to-one orthologs (Figure 3 in the main text considers all types of orthologs). The numbers in parentheses represent the counts of genes in the respective gene families. (a) gene families containing *H. sapiens* and *M. musculus* proteins, and (b) gene families containing *S. cerevisiae* and *S. pombe* proteins.

Table S1: Number of genes from human-mouse forming gene families, homologous pairs and number of families with different types of homologies.

Gene families (from gene trees)	8686	
genes making gene families	41501	(19,731 human + 21,770 mouse)
genes making homologous pairs	40912	(19,514 human + 21,398 mouse)
intersection (gene fams & hom pairs)	40,884	
protein coding genes	44,603	(22,376 human + 22,227 mouse)
intersection (p_coding genes & hom_genes)	40,722	
intersection (p_coding genes & gene families)	40,741	
total # of homologous pairs found in gene trees	21,8254	
ortholog pairs	24,106	
within species inparalog pairs	33,741	
within species outparalog pairs	88,625	
between specie outparalog pairs	71,782	
clusters containing homolgous pairs (at least 1 pair)		
ortholog pairs	8,606	99.07%
within inparalog pairs	1,299	14.95%
between outparalog pairs	3,205	36.89%
within outparalog pairs	3,249	37.40%
both within inparalog and ortholog pairs	1299	14.95%
both between homolog and within homolog	3,850	44.32%
ortholog only families	4,744	55.12%

Table S2: Number of genes from cerevisiae-pombe forming gene families, homologous pairs and number of families with different types of homologies.

Gene families (from gene trees)	3,061	
genes making gene families	7,335	(4,042 yeast + 3,293 pombe)
genes making homologous pairs	7,691	(4,208 yeast + 3,483 pombe)
intersection (gene fams & hom pairs)	7,334	
protein coding genes	11,839	(6,693 yeast + 5,146 pombe)
intersection (p_coding genes & hom_genes)	7,690	
intersection (p_coding genes & gene families)	3,061	
total # of homologous pairs found in gene trees	8,621	
ortholog pairs	3,249	
within species inparalog pairs	5,019	
within species outparalog pairs	202	
between specie outparalog pairs	151	
clusters containing homolgous pairs (at least 1 pair)		
ortholog pairs	2,488	81.33%
within inparalog pairs	999	32.60%
between outparalog pairs	94	3.00%
within outparalog pairs	130	4.20%
both within inparalog and ortholog pairs	463	15.12%
both between homolog and within homolog	1,079	35.27%
ortholog only families	1,969	64.03%

References

[1] G. Glazko, A. Gordon, and A. Mushegian. The choice of optimal distance measure in genome-wide datasets. *Bioinformatics*, 21(Suppl 3):iii3–iii11, 2005.

[2] A. Schlicker, F.S. Domingues, J. Rahnenfuhrer, and T. Lengauer. A new measure for functional similarity of gene products based on Gene Ontology. *BMC Bioinformatics*, 7:302, 2006.

[3] A. M. Altenhoff, R A. Studer, M. Robinson-Rechavi, and C. Dessimoz. Resolving the ortholog conjecture: orthologs tend to be weakly, but significantly, more similar in function than paralogs. *PLoS Comput Biol*, 8(5):e1002514, 2012.

[4] P. Resnik. Using information content to evaluate semantic similarity in a taxonomy. In *Proceedings of the 14th International Joint Conference on Artificial Intelligence*, pages 448–453, 1995.

[5] P. Radivojac, W. T. Clark, T. R. Oron, A. M. Schnoes, T. Wittkop, A. Sokolov, K. Graim, C. Funk, K. Verspoor, A. Ben-Hur, G. Pandey, J. M. Yunes, A. S. Talwalkar, S. Repo, M. L. Souza, D. Piovesan, R. Casadio, Z. Wang, J. Cheng, H. Fang, J. Gough, P. Koskinen, P. Toronen, J. Nokso-Koivisto, L. Holm, D. Cozzetto, D. W. Buchan, K. Bryson, D. T. Jones, B. Limaye, H. Inamdar, A. Datta, S. K. Manjari, R. Joshi, M. Chitale, D. Kihara, A. M. Lisewski, S. Erdin, E. Venner, O. Lichtarge, R. Rentzsch, H. Yang, A. E. Romero, P. Bhat, A. Paccanaro, T. Hamp, R. Kassner, S. Seemayer, E. Vicedo, C. Schaefer, D. Achten, F. Auer, A. Boehm, T. Braun, M. Hecht, M. Heron, P. Honigschmid, T. A. Hopf, S. Kaufmann, M. Kiening, D. Krompass, C. Landerer, Y. Mahlich, M. Roos, J. Bjorne, T. Salakoski, A. Wong, H. Shatkay, F. Gatzmann, I. Sommer, M. N. Wass, M. J. Sternberg, N. Skunca, F. Supek, M. Bosnjak, P. Panov, S. Dzeroski, T. Smuc, Y. A. Kourmpetis, A. D. van Dijk, C. J. ter Braak, Y. Zhou, Q. Gong, X. Dong, W. Tian, M. Falda, P. Fontana, E. Lavezzo, B. Di Camillo, S. Toppo, L. Lan, N. Djuric, Y. Guo, S. Vucetic, A. Bairoch, M. Linial, P. C. Babbitt, S. E. Brenner, C. Orengo, B. Rost, S. D. Mooney, and I. Friedberg. A large-scale evaluation of computational protein function prediction. *Nat Methods*, 10(3):221–227, 2013.

[6] Y. Jiang, T. R. Oron, W. T. Clark, A. R. Bankapur, D. D'Andrea, R. Lepore, C. S. Funk, I. Kahanda, K. M. Verspoor, A. Ben-Hur, C. E. Koo da, D. Penfold-Brown, D. Shasha, N. Youngs, R. Bonneau, A. Lin, S. M. Sahraeian, P. L. Martelli, G. Profiti, R. Casadio, R. Cao, Z. Zhong, J. Cheng, A. Altenhoff, N. Skunca, C. Dessimoz, T. Dogan, K. Hakala, S. Kaewphan, F. Mehryary, T. Salakoski, F. Ginter, H. Fang, B. Smithers, M. Oates, J. Gough, P. Toronen, P. Koskinen, L. Holm, C. T. Chen, W. L. Hsu, K. Bryson, D. Cozzetto, F. Minneci, D. T. Jones, S. Chapman, D. Bkc, I. K. Khan, D. Kihara, D. Ofer, N. Rappoport, A. Stern, E. Cibrian-Uhalte, P. Denny, R. E. Foulger, R. Hieta, D. Legge, R. C. Lovering, M. Magrane, A. N. Melidoni, P. Mutowo-Meullenet, K. Pichler, A. Shypitsyna, B. Li, P. Zakeri, S. ElShal, L. C. Tranchevent, S. Das, N. L. Dawson, D. Lee, J. G. Lees, I. Sillitoe, P. Bhat, T. Nepusz, A. E. Romero, R. Sasidharan, H. Yang, A. Paccanaro, J. Gillis, A. E. Sedeno-Cortes, P. Pavlidis, S. Feng, J. M. Cejuela,

T. Goldberg, T. Hamp, L. Richter, A. Salamov, T. Gabaldon, M. Marcet-Houben, F. Supek, Q. Gong, W. Ning, Y. Zhou, W. Tian, M. Falda, P. Fontana, E. Lavezzo, S. Toppo, C. Ferrari, M. Giollo, D. Piovesan, S. C. Tosatto, A. Del Pozo, J. M. Fernandez, P. Maietta, A. Valencia, M. L. Tress, A. Benso, S. Di Carlo, G. Politano, A. Savino, H. U. Rehman, M. Re, M. Mesiti, G. Valentini, J. W. Bargsten, A. D. van Dijk, B. Gemovic, S. Glisic, V. Perovic, V. Veljkovic, N. Veljkovic, E. S. D. C. Almeida, R. Z. Vencio, M. Sharan, J. Vogel, L. Kansakar, S. Zhang, S. Vucetic, Z. Wang, M. J. Sternberg, M. N. Wass, R. P. Huntley, M. J. Martin, C. O'Donovan, P. N. Robinson, Y. Moreau, A. Tramontano, P. C. Babbitt, S. E. Brenner, M. Linial, C. A. Orengo, B. Rost, C. S. Greene, S. D. Mooney, I. Friedberg, and P. Radivojac. An expanded evaluation of protein function prediction methods shows an improvement in accuracy. *Genome Biol*, 17(1):184, 2016.

[7] N. Zhou, Y. Jiang, T. R. Bergquist, A. J. Lee, B. Z. Kacsoh, A. W. Crocker, K. A. Lewis, G. Georghiou, H. N. Nguyen, M. N. Hamid, L. Davis, T. Dogan, V. Atalay, A. S. Rifaioglu, A. Dalkiran, R. Cetin Atalay, C. Zhang, R. L. Hurto, P. L. Freddolino, Y. Zhang, P. Bhat, F. Supek, J. M. Fernandez, B. Gemovic, V. R. Perovic, R. S. Davidovic, N. Sumonja, N. Veljkovic, E. Asgari, M. R. K. Mofrad, G. Profiti, C. Savojardo, P. L. Martelli, R. Casadio, F. Boecker, H. Schoof, I. Kahanda, N. Thurlby, A. C. McHardy, A. Renaux, R. Saidi, J. Gough, A. A. Freitas, M. Antczak, F. Fabris, M. N. Wass, J. Hou, J. Cheng, Z. Wang, A. E. Romero, A. Paccanaro, H. Yang, T. Goldberg, C. Zhao, L. Holm, P. Toronen, A. J. Medlar, E. Zosa, I. Borukhov, I. Novikov, A. Wilkins, O. Lichtarge, P. H. Chi, W. C. Tseng, M. Linial, P. W. Rose, C. Dessimoz, V. Vidulin, S. Dzeroski, I. Sillitoe, S. Das, J. G. Lees, D. T. Jones, C. Wan, D. Cozzetto, R. Fa, M. Torres, A. Warwick Vesztrocy, J. M. Rodriguez, M. L. Tress, M. Frasca, M. Notaro, G. Grossi, A. Petrini, M. Re, G. Valentini, M. Mesiti, D. B. Roche, J. Reeb, D. W. Ritchie, S. Aridhi, S. Z. Alborzi, M. D. Devignes, D. C. E. Koo, R. Bonneau, V. Gligorijevic, M. Barot, H. Fang, S. Toppo, E. Lavezzo, M. Falda, M. Berselli, S. C. E. Tosatto, M. Carraro, D. Piovesan, H. Ur Rehman, Q. Mao, S. Zhang, S. Vucetic, G. S. Black, D. Jo, E. Suh, J. B. Dayton, D. J. Larsen, A. R. Omdahl, L. J. McGuffin, D. A. Brackenridge, P. C. Babbitt, J. M. Yunes, P. Fontana, F. Zhang, S. Zhu, R. You, Z. Zhang, S. Dai, S. Yao, W. Tian, R. Cao, C. Chandler, M. Amezola, D. Johnson, J. M. Chang, W. H. Liao, Y. W. Liu, S. Pascarelli, Y. Frank, R. Hoehndorf, M. Kulmanov, I. Boudellioua, G. Politano, S. Di Carlo, A. Benso, K. Hakala, F. Ginter, F. Mehryary, S. Kaewphan, J. Bjorne, H. Moen, M. E. E. Tolvanen, T. Salakoski, D. Kihara, A. Jain, T. Smuc, A. Altenhoff, A. Ben-Hur, B. Rost, S. E. Brenner, C. A. Orengo, C. J. Jeffery, G. Bosco, D. A. Hogan, M. J. Martin, C. O'Donovan, S. D. Mooney, C. S. Greene, P. Radivojac, and I. Friedberg. The CAFA challenge reports improved protein function prediction and new functional annotations for hundreds of genes through experimental screens. *Genome Biol*, 20(1):244, 2019.